SCIENTIFIC REPORTS

OPEN

SUBJECT AREAS:
CANCER IMMUNOTHERAPY
CELLULAR IMMUNITY
TUMOUR IMMUNOLOGY
BIOMATERIALS

Received
9 April 2013

Accepted
27 June 2013

Published
16 July 2013

Correspondence and requests for materials should be addressed to X.P.W. (xp-wang@aist.go.jp); X.L. (lixia6969@hotmail.com) or A.I. (atsuo-ito@aist.go.jp)

* These authors contributed equally to this work.

Zn- and Mg- Containing Tricalcium Phosphates-Based Adjuvants for Cancer Immunotherapy

Xiupeng Wang[1]*, Xia Li[1]*, Kazuo Onuma[1], Yu Sogo[1], Tadao Ohno[2] & Atsuo Ito[1]

[1]Human Technology Research Institute, National Institute of Advanced Industrial Science and Technology (AIST), Central 6, 1-1-1 Higashi, Tsukuba, Ibaraki 305-8566, Japan, [2]School of Life Dentistry at Tokyo, The Nippon Dental University, Fujimi, Chiyoda-ku Tokyo 102-0071, Japan.

Zn-, and Mg-containing tricalcium phosphates (TCPs) loaded with a hydrothermal extract of a human tubercle bacillus (HTB) were prepared by immersing Zn-TCP and Mg-TCP in HTB-containing supersaturated calcium phosphate solutions. The *in vitro* and *in vivo* immunogenic activities of the HTB-loaded Zn-, and Mg-TCPs (Zn-Ap-HTB and Mg-Ap-HTB, respectively) were evaluated as potential immunopotentiating adjuvants for cancer immunotherapy. The Zn-Ap-HTB and Mg-Ap-HTB adjuvants showed no obvious cytotoxicity and more effectively stimulated granulocyte-macrophage colony-stimulating factor (GM-CSF) secretion by macrophage-like cells than unprocessed HTB or HTB-loaded TCP (T-Ap-HTB) *in vitro*. Zn-Ap-HTB and Mg-Ap-HTB mixed with liquid-nitrogen-treated tumor tissue markedly inhibited the *in vivo* development of rechallenged Lewis lung carcinoma (LLC) cells compared with T-Ap-HTB and the unprocessed HTB mixed liquid-nitrogen-treated tumor tissue. Zn-Ap-HTB and Mg-Ap-HTB contributed to eliciting potent systemic antitumor immunity *in vivo*.

The use of cancer vaccines attempts to harness the exquisite power and specificity of the immune system for cancer treatment[1]. The crucial point for cancer vaccines is the inclusion of an appropriate adjuvant (composed of immunopotentiators and delivery systems) to trigger an antitumor immune response (includes innate and adaptive immune responses)[1,2], because tumor cells (i) show reduced antigen presentation; and (ii) downregulate the immune responses of the body[1,3].

Pathogen-associated molecular patterns (PAMPs) are one of the most potent classes of immunopotentiating adjuvants. In particular, a hydrothermal extract of a human tubercle bacillus (HTB) has been studied for several decades for its clinical application to cancer therapy following radiation therapy; it is clinically used to recover leucocytes of cancer patients after radiation therapy. HTB is a mixture composed mainly of several polysaccharides[4]; it exhibits an immunostimulatory effect, exerts an antitumor response[5,6] and inhibits tumor metastasis[7]. For example, HTB induces the production of interleukin (IL)-12, IL-2, interferon (IFN)-γ[8], colony-stimulating factor (CSF) and IL-3, activates macrophages, improves T cell responses from type 2 helper T cells (Th2, antibody immunity) to type 1 helper T cells (Th1, cell-mediated immunity) response and restores the balance of Th1/Th2 cell responses[8]. However, unprocessed HTB is rapidly degraded in the extracellular environment and not efficient for use as a cancer adjuvant alone.

To enhance the immunopotentiating effect of HTB, a promising strategy is to achieve a sustained release of HTB using a delivery system[9–13], through which a synergistic effect between the principal components of adjuvants, i.e., the immunopotentiator and delivery system, is achieved. As for the conventional vaccine for human use, alum and calcium phosphate, have been approved by many countries. Calcium phosphate is a safe material for a delivery system, since it is a normal constituent of the body, and is well tolerated and readily resorbed by the body[14]. However, for cancer vaccines, the immunopotentiating property of calcium phosphate remains unsatisfactory. Thus it is possible to use tricalcium phosphate (TCP) as a material for the delivery system in two ways: one is as a carrier (vehicle) of HTB and the other is as a reservoir of biologically active elements, especially divalent cations.

Zinc (Zn) is an essential trace element in the human body. It promotes the activity of antigen presenting cells (APCs), such as macrophages[15], and Th1 cell responses[16]. Magnesium (Mg) is the fourth major cation in the human body and the second most prevalent intracellular cation. It plays important roles in determining the characteristics of macrophages, such as the regulation of cellular morphology, lysosomal enzyme release and

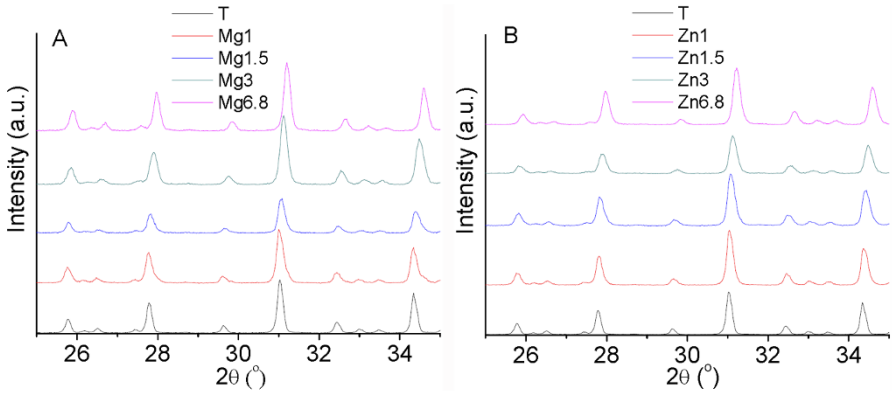

Figure 1 | XRD patterns of TCP, Mg-TCP (A) and Zn-TCP (B) powders.

phagocytosis[17]. Since both Zn and Mg can be easily incorporated in the crystal structure of TCP[18–20], the delivery of Zn and Mg to APCs should be possible with TCP. In this study, we hypothesized that Zn-, and Mg-containing TCPs (Zn-TCP and Mg-TCP, respectively) act as promising delivery systems for the hydrothermal extract of HTB and are more effective immunopotentiating adjuvants than a simple composite of HTB and TCP.

Results

Characterization of TCP, Mg-TCP and Zn-TCP before and after loading HTB. Figure 1 shows the XRD patterns of TCP, Mg-TCP or Zn-TCP powders. No extra reflection peaks attributed to impurity phases appeared in the XRD patterns of Mg-TCP and Zn-TCP powders. The substitution of Mg^{2+} or Zn^{2+} for Ca^{2+} in the TCP structure was confirmed by positional shifts of the diffraction peaks toward a higher angle, which corresponds to decreases in lattice constants with increasing Mg or Zn content. All the powders loaded with HTB containing supersaturated calcium phosphate solution showed no detectable change compared with those before loading, because the peaks attributed to coprecipitated apatite were broad and extremely weak owing to the small quantity and low crystallinity of apatite (data not shown).

Figures 2 and S2–S4 show the hydrodynamic radius of TCP, Mg-TCP and Zn-TCP particles measured by the dynamic light scattering technique. The average hydrodynamic radii of TCP, Mg-TCP and Zn-TCP particles were approximately 500–600 nm at various incidence angles of the laser (from 30–100°). These results suggest that the size of the particles was uniform in every direction. Figure S5 shows the EDX spectra of TCP, Mg-TCP and Zn-TCP powders. Mg and Zn peaks were obviously observed in Mg-TCP and Zn-TCP powders, respectively. Because the doped amounts of Mg or Zn are low, the peaks of Ca, P and O were similar. The intensity of Mg and Zn increased with increase of Mg and Zn content in Mg-TCP or Zn-TCP powders, respectively. The EDX is not a precise method to quantitatively analyze the element contents. The contents of Mg and Zn in Mg-TCP and Zn-TCP powders were further analyzed by ICP (Table S1). The Zn to Ca mol ratio in Zn1, Zn1.5, Zn3 and Zn6.8 was 0.93% ± 0.01%, 1.32% ± 0.03%, 2.91% ± 0.02% and 6.40% ± 0.02%, respectively. The Mg to Ca ratio in Mg1, Mg1.5, Mg3 and Mg6.8 was 0.88% ± 0.1%, 1.49% ± 0.02%, 2.98% ± 0.05% and 6.52% ± 0.05%, respectively. The zeta potentials of TCP, Mg1.5 and Zn1.5 particles were evaluated as −14.11, −17.16 and −18.32 mV, respectively, from the electric mobility distributions of these particles, as showed in Fig. 3. The solutions of TCP, Mg1.5 and Zn1.5 particles may be unstable. Therefore, before loading HTB, the solutions of TCP, Mg1.5 and Zn1.5 particles were dispersed with ultrasonic for 1 h. Moreover, during the process of loading HTB onto the various TCP powders, the reaction was conducted under continuous stirring at a speed of about 200 rpm.

Figure 4 shows FESEM images of typical TCP, Mg-TCP and Zn-TCP powders before and after being loaded with HTB. Before loading, the powders consisted of round grains with a smooth surface. After loading, the powder exhibited a relatively rough surface, probably owing to the initial dissolution on grain surfaces and at grain boundaries, and the subsequent formation of nanosized precipitates.

Figure S6 show the FTIR spectra of the samples. HTB showed the C-H stretching vibration at 2926 cm^{-1}, amide I (mainly C=O stretching vibration) at 1600–1660 cm^{-1} and amide II (mainly N–H bending vibration) at 1480–1570 cm^{-1}. TCP showed its characteristic absorption bands of the ν_4 PO_4 mode at 500–650 cm^{-1} and those of the ν_3 PO_4 mode at 900–1200 cm^{-1}. TCP after immersing in RSM without HTB (T-Ap) showed additional absorption bands at about 870 and 1390–1590 cm^{-1}. TCP after immersing in HTB-containing RSM (T-Ap-HTB) exhibited broad adsorption bands at

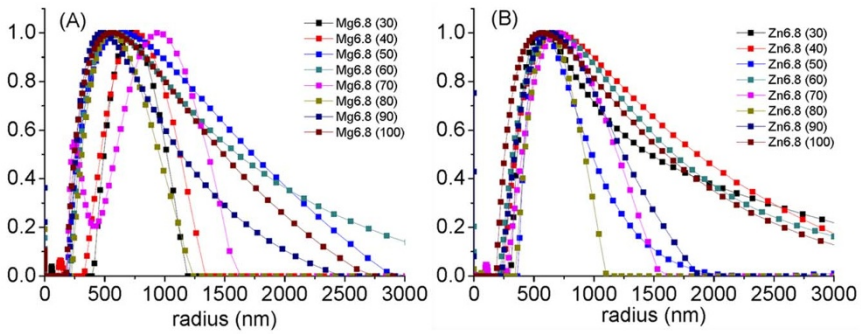

Figure 2 | Distributions of hydrodynamic radius of Mg6.8 (A) and Zn6.8 (B) dispersed in PBS(-) obtained by dynamic light scattering measurement at various incidence angles of laser (from 30–100°).

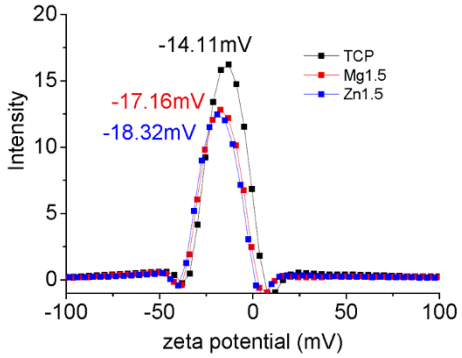

Figure 3 | Electrical mobility distributions of TCP, Mg1.5 and Zn1.5 particles in PBS(-).

2926 cm^{-1} (mainly C–H stretching vibration), 1480–1700 cm^{-1} (mainly C=O stretching vibration and N–H bending vibration) and 1330–1500 cm^{-1} (mainly CO_3^{2-} vibration), which suggests the coprecipitation of HTB and the formation of CO_3^{2-}-substituted apatite on the TCP particles. The other samples after immersing in HTB-containing RSM, such as Mg1-Ap-HTB, Mg1.5-Ap-HTB, Mg3-Ap-HTB, Mg6.8-Ap-HTB, Zn1-Ap-HTB, Zn1.5-Ap-HTB, Zn3-Ap-HTB and Zn6.8-Ap-HTB, all showed similar adsorption bands to T-Ap-HTB.

In the RSM, the concentrations of TCP, Zn-TCP or Mg-TCP particles were all fixed to be 0.15 mg/mL. After coprecipitation, the amount of newly formed apatite was calculated as 0.06–0.08 mg per 0.15 mg of particles with a Ca/P molar ratio of 1.6–1.8 regardless of the Mg or Zn content of the particles, according to the assay using ICP spectrophotometry. It was inferred that 10 ~ 20% HTB in the RSM coprecipitated with the newly formed apatite on Zn-TCP and Mg-TCP.

***In vitro* immunogenic activity of T-Ap-HTB, Mg-Ap-HTB, and Zn-Ap-HTB adjuvants.** Figure 5 shows the amount of GM-CSF secreted by macrophage-like cells in the original culture medium as well as in the culture media containing unprocessed HTB, lipopolysaccharide (LPS), T-Ap-HTB, Mg-Ap-HTB, and Zn-Ap-HTB. The original culture medium, and unprocessed HTB-containing and LPS-containing culture media were used as controls. Only negligible immunogenic activity was observed for unprocessed HTB since there was no difference in GM-CSF concentration between the original culture medium and the medium with unprocessed HTB. As a whole, Mg-Ap-HTB and Zn-Ap-HTB enhanced GM-CSF secretion by the macrophage-like cells compared with T-Ap-HTB. Zn1.5-Ap-HTB induced the highest GM-CSF secretion level at 1 μg/mL. Meanwhile, Mg1.5-Ap-HTB induced the second highest GM-CSF secretion level at 1 μg/mL.

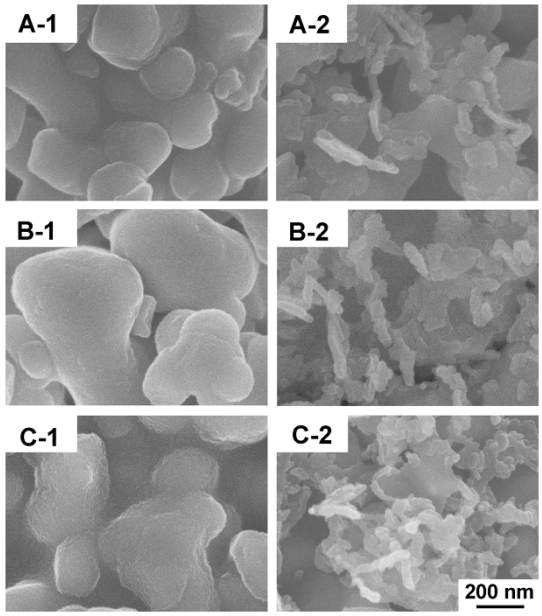

Figure 4 | FESEM images of TCP (A-1), Mg1.5 (B-1), Zn1.5 (C-1), T-Ap-HTB (A-2), Mg1.5-Ap-HTB (B-2) and Zn1.5-Ap-HTB (C-2).

The immunogenic activity test of Mg-Ap-HTB and Zn-Ap-HTB adjuvants was repeated in the absence of LPS, and T-Ap-HTB. Similar with Figure 5, Mg-Ap-HTB and Zn-Ap-HTB enhanced GM-CSF secretion by the macrophage-like cells compared with unprocessed HTB. Mg1.5-Ap-HTB and Zn1.5-Ap-HTB induced the higher GM-CSF secretion level compared with TCP, Zn-, and Mg-TCPs with different Mg or Zn contents (data not shown). Thus, Mg1.5-Ap-HTB and Zn1.5-Ap-HTB were selected for the subsequent in vivo immunogenic activity test.

Cytotoxicity of T-Ap-HTB, Mg-Ap-HTB, and Zn-Ap-HTB adjuvants. Figure 6 shows the *in vitro* viabilities of the macrophage-like cells cultured in the original culture medium as well as in the culture media containing T-Ap-HTB, Mg-Ap-HTB, and Zn-Ap-HTB adjuvants. Below 10 μg/mL, T-Ap-HTB, Mg-Ap-HTB, and Zn-Ap-HTB adjuvants did not significantly affect the viability of the macrophage-like cells as compared with the original culture medium. According to the results, the cytotoxicity of the adjuvants was negligible at a particle concentration below 10 μg/mL.

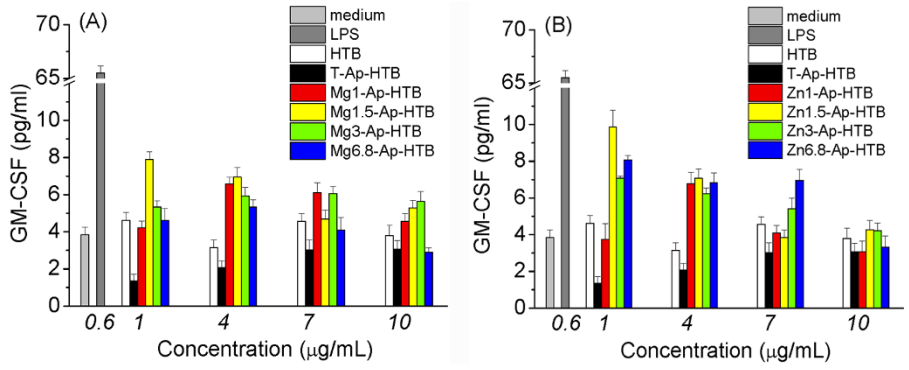

Figure 5 | GM-CSF secretion by macrophage-like cells after cultured in the original culture medium, culture media containing HTB, Mg-Ap-HTB (A), and Zn-Ap-HTB (B) adjuvants (n=8).

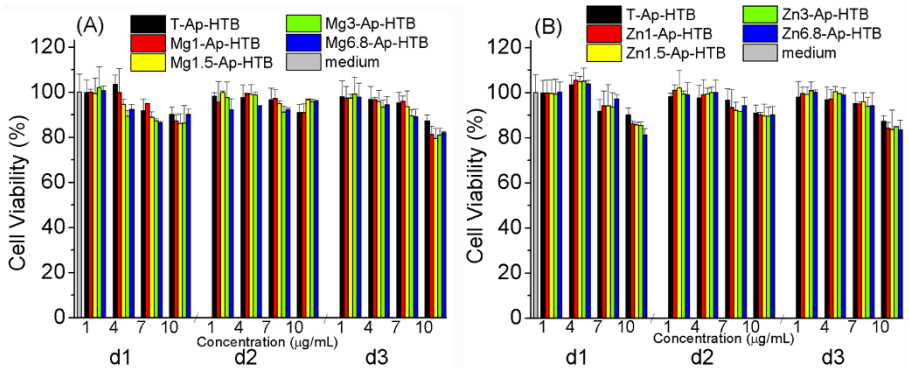

Figure 6 | ***In vitro*** **cell viability of macrophage-like cells after cultured in the original culture medium, culture media containing T-Ap-HTB, Mg-Ap-HTB (A), and Zn-Ap-HTB (B) adjuvants (n=3*2).**

Ion release. Figures S7 and S8 show the Ca, P, Mg or Zn concentrations of ultrapure water after immersing T-Ap, Zn-Ap, or Mg-Ap particles at particle concentrations of 1, 4 and 10 μg/mL for 5, 20 and 42 h. With an increase in the Mg content of Mg-Ap and an increase in particle concentration, the amount of Mg^{2+} released increased. However, the increase in the Mg content of Mg-Ap was associated with decreases in the amounts of Ca and P released. With an increase in immersion time, Mg^{2+} concentration also increased. Zn-Ap showed similar trends to Mg-Ap.

In vivo **immunogenic activity and cytokine secretion in mice spleen.** For the *in vivo* immunogenic activity test, Mg1.5-Ap-HTB and Zn1.5-Ap-HTB adjuvants were used depending on the *in vitro* results. T-Ap-HTB and unprocessed HTB were also examined as controls in this study. The *in vivo* test was done twice.

At the first time, the test was carried out using 20 mice in total (6-week-old, female, C57BL/6J, CLEA Inc., Japan). The mice were randomly divided into 4 groups (5 mice per group) according to the type of sample to be injected. There were no critical differences among different groups for the volumes of tumors formed in the injection site 10 days after the first injection of LLC cells. The tumor volumes were approximately 50–250 mm^3 (Fig. S9). Eight days after the re-challenge of LLC cells, tumor formation was observed in all groups. The inhibitory ratio against tumor formation in different groups was calculated. On the 8th day, the highest inhibitory ratio against tumor formation was achieved in the Zn1.5-Ap-HTB group (80%). The inhibitory ratios of tumor formation for the groups of unprocessed HTB, T-Ap-HTB and Mg1.5-Ap-HTB were 40, 60 and 60%, respectively. On the 12th day, the inhibitory ratio against tumor formation was still higher for Zn1.5-Ap-HTB group than for the other groups. On the last day of the observation (29th day), the inhibitory ratio against tumor formation remained 60% for the Zn1.5-Ap-HTB group, while those of the other groups simultaneously decreased to 20% (Fig. S10). The final mean tumor volumes for the unprocessed HTB, T-Ap-HTB, Mg1.5-Ap-HTB and Zn1.5-Ap-HTB groups were 694.0 ± 584.4, 14.3 ± 13.8, 293.1 ± 324.9 and 4.8 ± 10.7 mm^3, respectively (Fig. S11). The degree of secretion of GM-CSF, IL-2, TNFα, IL-12 and IFNγ in the mouse spleen after the re-challenge of LLC cells was measured using ELISA kits. Although the Zn1.5-Ap-HTB and Mg1.5-Ap-HTB groups showed higher amount of GM-CSF, IL-2, TNFα, IL-12 and IFNγ in mouse spleen than unprocessed HTB and T-Ap-HTB group, no significant difference was observed due to the small amount of mice numbers in each group (data not shown).

To further confirm the immunogenic activity of the adjuvant, the experiment was repeated. At the second time, the test was carried out using 48 mice in total (6-week-old, female, C57BL/6J, CLEA Inc., Japan). The mice were randomly divided into 4 groups (12 mice per group) according to the type of sample to be injected. There were no critical differences among different groups for the volumes of tumors formed in the injection site 7 days after the first injection of LLC cells. The tumor volumes were approximately 110–200 mm^3 (Fig. S12). This result suggested that the innate immunities of all the mice against LLC cells were almost same and that individual differences in innate immunity were negligible. Nine days after the re-challenge of LLC cells, the highest inhibitory ratio against tumor formation was achieved in the Zn1.5-Ap-HTB and Mg1.5-Ap-HTB group (66.7%, Fig. 7). On the 9th day, the inhibitory ratios of tumor formation for the groups of unprocessed HTB and T-Ap-HTB were 16.7 and 25%, respectively. On the last day of the observation (29th day), the inhibitory ratio against tumor formation was 40% for the Zn1.5-Ap-HTB group, 33.3% for Mg1.5-Ap-HTB group, 16.7 for T-Ap-HTB group and 8.3% for unprocessed HTB group (Fig. 7). The final mean tumor volumes for the unprocessed HTB, T-Ap-HTB, Mg1.5-Ap-HTB and Zn1.5-Ap-HTB groups were 565 ± 489, 370 ± 330, 122 ± 103 and 94 ± 138 mm^3, respectively (Fig. S13). The degree of secretion of GM-CSF, IL-2, TNFα, IL-12 and IFNγ in the mouse spleen after the re-challenge of LLC cells was also repeated (Fig. 8). The Zn1.5-Ap-HTB and Mg1.5-Ap-HTB groups showed high GM-CSF, IL-2, TNFα, IL-12 and IFNγ amounts in mouse spleen. The Zn1.5-Ap-HTB group showed significantly higher GM-CSF, IL-2, TNFα, IL-12 and IFNγ amounts in mouse spleen than unprocessed HTB and T-Ap-HTB group (Fig. 8). From the viewpoint of the inhibitory effect of tumor growth as one of the immunological functions, Zn-Ap-HTB and Mg-Ap-HTB showed promise as an adjuvant for preventing tumor recurrence in cancer immunotherapy.

Discussion

The Zn-TCP- and Mg-TCP-based adjuvants (Zn-Ap-HTB or Mg-Ap-HTB adjuvants) markedly induced *in vitro* GM-CSF secretion by the macrophage-like cells, and the Zn-TCP-based adjuvant most efficiently inhibited *in vivo* tumor development using re-challenged

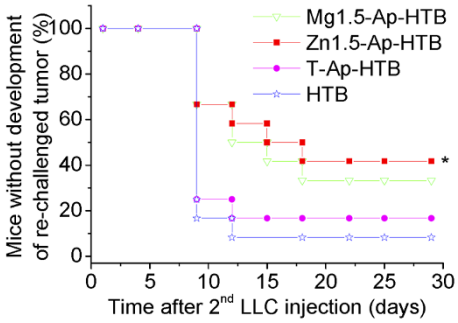

Figure 7 | **Percent of mice without development of re-challenged tumor on the right flank of mice over time after re-challenge of LLC cells.** (* $P<0.05$ vs. HTB group, n=12).

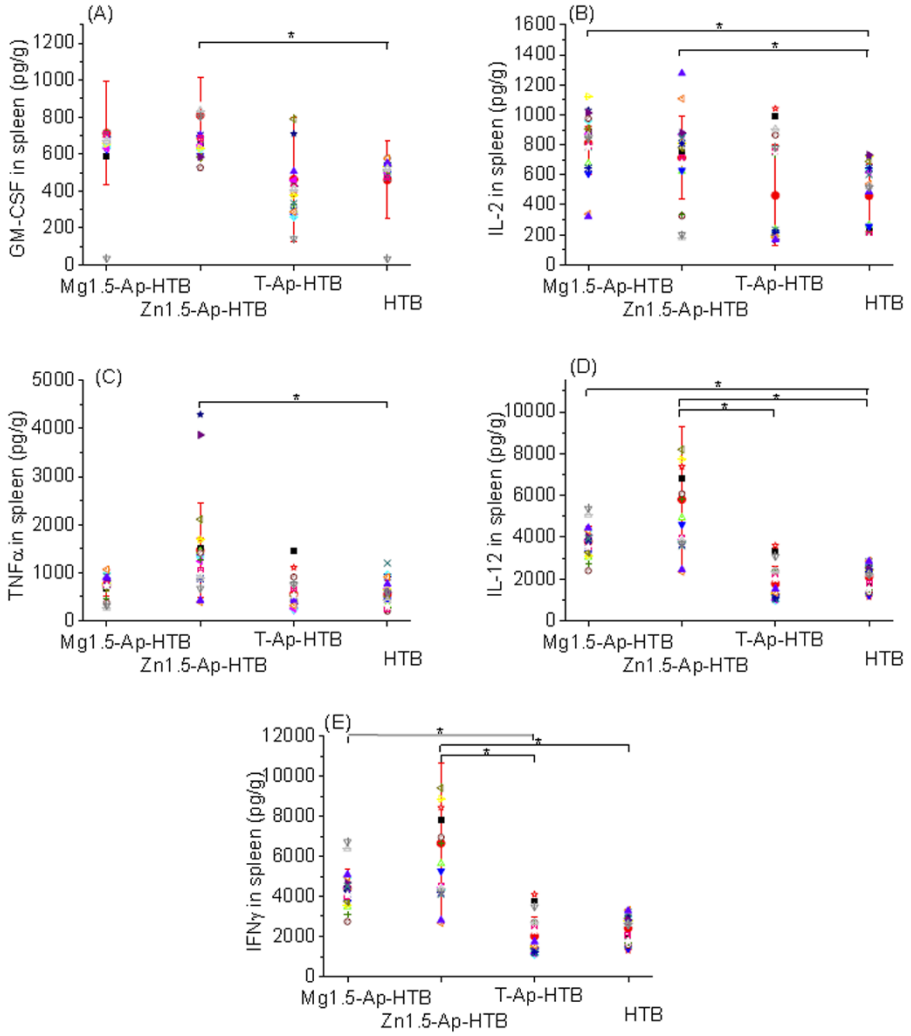

Figure 8 | Contents of cytokines relating to cell-mediated immunity in mice spleen after 29 days from re-challenge of LLC cells. GM-CSF (A), IL-2 (B), TNFα (C), IL-12 (D) and IFNγ (E). Red solid circles with error bars show the mean value and standard deviation (* $p<0.05$, $n=12$).

LLC cells in combination with a liquid-nitrogen-treated autologous tumor tissue. Possible reasons for the marked efficiency of Zn-Ap-HTB or Mg-Ap-HTB adjuvants include the presence of particles as depots of HTB as the immunopotentiator, the release of Zn (or Mg) ions and the decrease in the solubility of tricalcium phosphate with the addition of Zn (or Mg) ions, all of which may subsequently result in an increase in the degree of secretion of cytokines (e.g., GM-CSF, IL-2, TNFα, IL-12 and IFNγ) and the increase in cell-mediated immunity.

Using an HTB-containing supersaturated calcium phosphate solution, HTB-apatite composites were formed on the surface of Zn-TCP and Mg-TCP by consuming calcium and phosphate ions (Figs. 4 and S6). HTB is considered to precipitate on the surface or in interstices of apatite to from HTB-apatite composites[21–25]. The presence of Zn or Mg in TCP affects the coprecipitation of apatite in two ways. One is that the release of Zn or Mg from TCP particles would inhibit the precipitation of low-crystallinity apatite[26]. The other is that, the presence of Zn or Mg leads to a decrease in the solubility of tricalcium phosphate[19,20], thus facilitating the precipitation of low-crystallinity apatite on Zn-, and Mg-TCP compared with that on pure TCP.

The release of Zn^{2+} or Mg^{2+} from the Zn-Ap-HTB or Mg-Ap-HTB adjuvant promoted GM-CSF secretion by the macrophage-like cells *in vitro* and inhibited the development of the re-challenged tumor *in vivo* (Figs. 5, 7 and S10–S13). With 1–10 μg/mL Zn, and Mg-TCP particles in ultrapure water, the amount of Zn or Mg released is 0 ~ 0.055 or 0 ~ 0.02 ppm (Figs. S7 and S8), respectively. Zn depletion causes immune cell dysfunctions, while Zn supplementation can either restore the function in the setting of dysfunction or improve normal immune cell function[15,27,28]. For example, Zn positively mediates the gene expressions of IL-2 and IFN-γ in the Th1 cell line[16]. On the other hand, Zn deficiency adversely affects T cell proliferation, decreases the production of Th1 cell cytokines, such as IFN-γ, IL-2, and TNF-α, shifts the Th1 response to the Th2 response and results in an imbalance in the Th1/Th2 cell response[27,29]. Therefore, the results shown in Fig. S8 can reasonably explain the high degree secretion of cytokines for cell-mediated immunity in the Zn1.5-Ap-HTB-injected mice. Mg plays an important role in determining the characteristics of macrophages, such as morphology, lysosomal enzyme release and phagocytosis[17].

The decrease in the solubility of TCP with the substitution of Zn^{2+} or Mg^{2+} is another reason for the increase in the degree of *in vitro* GM-CSF secretion from the macrophage-like cells and for the *in vivo* inhibition of the development of the re-challenged tumor (Figs. 5, 7 and S10–S13). The equilibrium solubility of Mg-TCP (or Zn-TCP) decreased with increasing Zn (or Mg) content[19,20]. The decrease in solubility can be attributed to the increased stability of the TCP structure caused by the substitution of Zn^{2+} or Mg^{2+}. The decrease in solubility facilitates macrophage activation. For example, HA particles of low solubility caused a stronger induction of GM-CSF secretion from human peripheral blood mononuclear cells (with the

potential to differentiate to macrophages and dendritic cells) than beta-TCP particles of high solubility[30].

The surgically removed tumor tissue was treated with liquid nitrogen to utilize it as an autologous tissue antigen. The treatment of a tumor tissue with liquid nitrogen in this study can be easily replaced with cryosurgery in clinical application, which is a highly efficient, minimally invasive method by the in situ freezing of tumor tissue. The proteins released from the liquid-nitrogen-treated tumor tissue may initiate a specific antitumor immune response, induce the tumor regression and inhibit secondary growth of the tumor[31]. However, note that both immunostimulatory and immunosuppressive responses may be triggered by the liquid-nitrogen-treated tumor tissue depending on the type of cytokine released by APCs and other cells within the microenvironment[31]. In this study, the Zn-Ap-HTB and Mg-Ap-HTB adjuvants significantly stimulated the secretion of cytokines (e.g., GM-CSF, IL-2, TNFα, IL-12 and IFNγ) in the mouse spleen (Fig. 8), which trigger the immunostimulatory response against tumors through cell-mediated immunity. In more detail, GM-CSF can increase the number of immature DCs at injection sites, stimulate DC recruitment and maturation and enhance tumor immunogenicity, thus stimulate antitumor immune responses[32]. IL-2 is necessary for the development of T cell immunologic memory, which depends on the improvement in the number and function of antigen-selected T cell clones[33,34]. TNF-α can induce apoptotic cell death and inflammation, and inhibit tumorigenesis[35,36]. IL-12 is a T cell-stimulating factor that stimulates the growth and function of T cells, as well as the production of IFNγ and TNFα from T, and mediates the enhancement of the cytotoxic activity of NK cells and CD^{8+} cytotoxic T lymphocytes[37]. IFN-γ has immunoregulatory and antitumor properties. In conjunction with TNF, IFN-γ has direct cytotoxic effects on tumor cells[38].

Note that the stimulatory effects of HTB and Zn-TCP or Mg-TCP on immune cells are concentration-dependent: an initial increase in the concentration of HTB and Zn-TCP or Mg-TCP induces cytokine production by macrophages, but further increase has an opposite effect. Note that the long-term administration of HTB at a high dose results in a weaker antitumor effect and a shorter survival time in the case of stage IIIb cervical cancer than that at a low dose[39]. Similarly, the effects of Zn on immune functions strongly depend on its concentration[40]. An initial increase in Zn concentration induces an improvement in monocyte and T-cell functions, but further increase in concentration leads to suppression[40]. Therefore, the doses of HTB, Zn and Mg in the Zn-Ap-HTB and Mg-Ap-HTB adjuvants should be further studied to optimize antitumor immune stimulation.

To conclude, Zn-Ap-HTB and Mg-Ap-HTB adjuvants were prepared by immersing Zn-TCP and Mg-TCP in HTB-containing supersaturated calcium phosphate solutions. The Zn-Ap-HTB and Mg-Ap-HTB adjuvants, particularly the Mg1.5-Ap-HTB and Zn1.5-Ap-HTB adjuvants, strongly induced *in vitro* GM-CSF secretion by macrophage-like cells. The Zn1.5-Ap-HTB and Mg1.5-Ap-HTB adjuvants combined with liquid-nitrogen-treated tumor tissue elicited a more potent systemic antitumor immunity that inhibited the *in vivo* development of a re-challenged tumor than T-Ap-HTB adjuvants and unprocessed HTB. Thus, Zn-Ap-HTB and Mg-Ap-HTB adjuvants may be effective for cancer immunotherapy for inhibiting tumor recurrence.

Methods

TCP, Mg-TCP and Zn-TCP particle preparation. The starting materials for preparing various TCP powders were powders of pure βTCP, Mg-TCP with 6.8 mol% Mg and Zn-TCP with 11.8 mol% Zn. Mg-TCP (1.0, 1.5, and 3 mol% Mg) and Zn-TCP (1.0, 1.5, 3, and 6.8 mol% Zn) powders were prepared by mixing pure βTCP powder with either Mg-TCP with 6.8 mol% Mg or Zn-TCP with 11.8 mol% Zn, and then grinding and heating the mixture at 850°C for 1 h. The obtained powders were designated as Mg1, Mg1.5, Mg3, Zn1, Zn1.5, Zn3 and Zn6.8, respectively. Pure βTCP powder and Mg-TCP with 6.8 mol% Mg were also treated by the same procedure and designated as T and Mg6.8, respectively.

Loading hydrothermal extract of a human tubercle bacillus (HTB) on TCP, Mg-TCP and Zn-TCP powders. All the solutions used for loading the hydrothermal extract of HTB on TCP, Mg-TCP and Zn-TCP powders were infusion fluids clinically available in Japan. The hydrothermal extract of HTB (Ancer® S.C. Injection solution, Zeria Pharma Co., Ltd., Japan) was aseptically concentrated five times in a water bath at 100°C before use (hereafter, the solution is labeled as five-times-concentrated Ancer). Ringer's solution (Otsuka Pharmaceutical Co., Ltd, 2.25 mM Ca^{2+}), Solita®-T No. 2 (Ajinomoto Pharmaceuticals Co., Ltd., Japan, 10 mM PO_4^{3-}) and an alkalinizer (Meylon® injection 7%, Otsuka Pharmaceutical Co., Ltd, 833 mM $NaHCO_3$) were used at their original concentrations.

The process of loading HTB onto the various TCP powders was carried out aseptically as follows: a supersaturated calcium phosphate solution, designated as RSM hereafter, was prepared by mixing Ringer's solution, Solita®-T No. 2 and Meylon® as shown in previous publication[41]. Three mg of TCP, Zn-TCP or Mg-TCP powders was sterilized at 160°C for 3 h, dispersed into 150 μL of RSM solution and sonicated for suspension. Then, 2 mL of the supersaturated RSM was supplemented with 200 μL of 5-times-concentrated Ancer and 15 μL of the above suspension. HTB was loaded onto the TCP particles by coprecipitation with low-crystallinity apatite (Ap). The coprecipitation reaction was conducted under continuous stirring at a speed of about 200 rpm at 25°C for 1 day. After centrifugal separation and freeze-drying, the obtained samples were designated as T-Ap-HTB, Mg1-Ap-HTB, Mg1.5-Ap-HTB, Mg3-Ap-HTB, Mg6.8-Ap-HTB, Zn1-Ap-HTB, Zn1.5-Ap-HTB, Zn3-Ap-HTB and Zn6.8-Ap-HTB. The samples prepared under the same conditions without HTB were designated as T-Ap, Mg1-Ap, Mg1.5-Ap, Mg3-Ap, Mg6.8-Ap, Zn1-Ap, Zn1.5-Ap, Zn3-Ap and Zn6.8-Ap.

Physiochemical characterizations. The morphology of powder particles was observed using a field-emission scanning electron microscope (FESEM, S-4800, Hitachi, Japan) at an acceleration voltage of 10 kV after being coated with platinum. The contents of Mg and Zn in Mg-TCP and Zn-TCP powders were analyzed by energy dispersive x-ray spectroscopy (EDX) and inductively coupled plasma atomic emission spectrometer (ICP: SPS7800, Seiko Instruments, Inc.), respectively. Crystalline phase was analyzed by X-ray diffraction (XRD) analysis using CuKα X-ray at 40 kV and 300 mA by powder X-ray diffractometry (Model RINT 2400; Rigaku, Japan). Fourier transform infrared spectrometry (FTIR) was carried out using an FTIR-350 spectrometer (JASCO Corporation, Japan) by the KBr pellet method. The RSM solution before and after coprecipitation was quantitatively analyzed for calcium and phosphorus using an inductively coupled plasma atomic emission spectrometry (ICP: SPS7800, Seiko Instruments, Japan). After immersing T-Ap, Zn-Ap, or Mg-Ap in ultrapure water at concentrations of 1, 4, and 10 μg/mL for 5, 20 and 42 h, calcium, phosphorus, magnesium or zinc concentration was also measured by ICP. Zeta potential was evaluated from the electrical mobility distribution of each particle using zeta-potential and particle size analyzer ELS-Z (Otsuka Electronics Co., Ltd., Osaka, Japan) by dispersing the samples in phosphate-buffered saline (PBS(-)) solution at 0.15 mg/mL. To measure the distribution of the hydrodynamic radius of as-prepared TCP, Mg-TCP and Zn-TCP particles, dynamic light scattering (DLS) measurement was performed by dispersing the particles in PBS(-) solution at 0.15 mg/mL with a multi angle DLS optical system (Otsuka Electronics Co., Ltd., Osaka, Japan) using a laser at a wavelength of 533 nm. The data was analyzed using ALV-Correlator Software (ALV Ltd., Germany).

***In vitro* immunogenic activity test.** To determine immunogenic activity, the amount of GM-CSF secreted by THP-1 cells (human lymphocyte-like cells, Riken Bio Resource Center, Japan) after differentiation into macrophage-like cells and in the presence of the sample powders was quantified *in vitro*. Firstly, 0.5 mL of THP-1 cell suspension (2×10^6 cells·mL^{-1}) was poured into a well of a 24-well cell culture plate and the cells were induced to differentiate into macrophage-like cells in a differentiation medium, i.e., RPMI1640 (Invitrogen, USA) supplemented with 10% fetal bovine serum (Invitrogen, USA) and 800 nM phorbol 12-myristate 13-acetate (PMA, Sigma, USA), for 4 days. Then; the cells that adhered on the cell culture wells, considered as macrophage-like cells, were washed twice with PBS(-) and precultured in 1 mL of fresh RPMI1640 without PMA for another day. After the preculture, the medium was changed to a medium with sample concentrations of 1–10 μg/mL. After a 40-h culture of the macrophage-like cells with the samples, the medium was analyzed for GM-CSF secreted by macrophage-like cells using a high-sensitivity (h)GM-CSF ELISA system (Thermo Fisher Scientific Inc. USA). Note that when samples can immunologically stimulate macrophage-like cells appropriately, the cells secrete a certain amount of GM-CSF in response to the stimulation. HTB, Mg-Ap-HTB, Zn-Ap-HTB adjuvants were tested simultaneously using the same set of cells.

The cytotoxicity test was performed as follows: After a 1d, 2d and 3d culture of the macrophage-like cells with the samples, the medium was taken out for the above ELISA test and a new medium was added. Then, the macrophage-like cells were counted using a CCK-8 kit (Dojindo Molecular Technologies, Japan) in accordance with the manufacturer's instructions. HTB, Mg-Ap-HTB, Zn-Ap-HTB adjuvants were tested simultaneously using the same set of cells.

***In vivo* immunogenic activity test.** The flowchart of the *in vivo* immunogenic activity test of the samples is shown in Fig. S1. The *in vivo* test was carried out following the three steps described below:

Step 1: Live Lewis lung carcinoma (LLC) cells (5×10^5 cells/mouse, Riken Bio Resource Center, Japan) were injected subcutaneously into the left flank of the mice. After 7-10 days, solid tumors formed in the regions where LLC cells were injected.

The tumor tissue was surgically removed from each mouse and immersed in liquid nitrogen for 30 min. Then, the tumor tissue was homogenized with a CryoMill (MM200, Retsch Co., Ltd., Germany) to be used as autologous tumor antigens for individual mice.

Step 2: 3, 7 and 14 days after the removal of the tumor tissue, 0.6 mg of Mg1.5-Ap-HTB, Zn1.5-Ap-HTB and T-Ap-HTB, or 0.8 μg of unprocessed HTB mixed with the homogenized tumor tissue were injected into the original tumor site; the samples were injected three times for each mouse. Tumor recurrence around the original tumor site was carefully observed twice a week until step 3.

Step 3: One month after step 1, live LLC cells (5×10^5 cells/mouse) were re-challenged subcutaneously into the right flank of the mice without tumor recurrence on the left side. Tumor development on the right flank in the re-challenged mice was monitored for 29 days. Percent of mice without development of re-challenged tumor on the right flank of mice was analyzed by a Kaplan–Meier log rank test. Differences were considered significant at $P<0.05$. To determine the cytokine or marker contents for cell-mediated immunity (GM-CSF, interleukin-2 (IL-2), tumor necrosis factor-α (TNFα), interleukin-12 (IL-12) and interferon-γ (IFNγ)) in the spleen, the spleen was excised and digested with a tissue protein extraction reagent (Thermo Fisher Scientific Inc. USA). The GM-CSF, IL-2, TNFα, IL-12 and IFNγ contents of the spleen were then determined with an ELISA system (Thermo Fisher Scientific Inc. USA). These cytokine contents were normalized by dividing them by the weight of the spleen. Contents of cytokines relating to cell-mediated immunity in mice spleen were analyzed by a Student's t-test. Differences were considered significant at $P<0.05$.

All the animal experiments were permitted by the Ethical Committee of the National Institute of Advanced Industrial Science and Technology (AIST), Japan. All the animal experiments and feeding were carried out in accordance with the guidelines of the Ethical Committee of the National Institute of Advanced Industrial Science and Technology (AIST), Japan.

1. Blattman, J. N. & Greenberg, P. D. Cancer immunotherapy: a treatment for the masses. *Science* **305**, 200–205 (2004).
2. Pashine, A., Valiante, N. M. & Ulmer, J. B. Targeting the innate immune response with improved vaccine adjuvant. *Nat Med* **11**, s63–s68 (2005).
3. Schreiber, R. D., Old, L. J. & Smyth, M. J. Cancer immunoediting: integrating immunity's roles in cancer suppression and promotion. *Science* **331**, 1565–1570 (2011).
4. Kobatake, H. *et al.* Studies on hot water extract of Mycobacterium-tuberculosis .1. Structural-analyses of polysaccharides. *Yakugaku Zasshi* **101**, 713–722 (1981).
5. Oka, H. *et al.* Z-100, an immunomodulatory arabinomannan extracted from Mycobacterium tuberculosis strain aoyama B, augments anti-tumor activities of X-ray irradiation against B16 melanoma in association with the improvement of type 1 T cell responses. *Biol Pharm Bull* **27**, 82–88 (2004).
6. Sasaki, H., Schmitt, D., Hayashi, Y., Pollard, R. B. & Suzuki, F. Antitumor mechanisms of Z-100, an immunomodulatory arabinomannan extracted from mycobacterium-tuberculosis - the importance of lymphocytes infiltrated into tumor sites. *Nat Immun* **12**, 104–112 (1993).
7. Kobayashi, M., Pollard, R. B. & Suzuki, F. Inhibition of pulmonary metastasis by Z-100, an immunomodulatory lipid-arabinomannan extracted from Mycobacterium tuberculosis, in mice inoculated with B16 melanoma. *Anti-Cancer Drug* **8**, 156–163 (1997).
8. Oka, H. *et al.* An immunomodulatory arabinomannan extracted from Mycobacterium tuberculosis, Z-100, restores the balance of Th1/Th2 cell responses in tumor bearing mice. *Immunol Lett* **70**, 109–117 (1999).
9. Eisenbarth, S. C., Colegio, O. R., O'Connor, W., Sutterwala, F. S. & Flavell, R. A. Crucial role for the Nalp3 inflammasome in the immunostimulatory properties of aluminium adjuvants. *Nature* **453**, 1122–U1113 (2008).
10. Ali, O. A., Huebsch, N., Cao, L., Dranoff, G. & Mooney, D. J. Infection-mimicking materials to program dendritic cells in situ. *Nature Materials* **8**, 151–158 (2009).
11. Wang, X., Li, X., Sogo, Y. & Ito, A. Simple synthesis route of mesoporous AlOOH nanofibers to enhance immune responses. *RSC Advances* **3**, 8164–8167 (2013).
12. Li, X. *et al.* Mesoporous silica-calcium phosphate-tuberculin purified protein derivative composites as an effective adjuvant for cancer immunotherapy. *Adv Healthc Mater*, http://dx.doi.org/10.1002/adhm.201200149 (2013).
13. Wang, X., Li, X., Ito, A., Sogo, Y. & Ohno, T. Particle-size-dependent toxicity and immunogenic activity of mesoporous silica-based adjuvants for tumor immunotherapy. *Acta Biomater* **9**, 7480–7849 (2013).
14. Gupta, R. K. *et al.* Adjuvants - a balance between toxicity and adjuvanticity. *Vaccine* **11**, 293–306 (1993).
15. Prasad, A. S. Zinc: role in immunity, oxidative stress and chronic inflammation. *Curr Opin Clin Nutr* **12**, 646–652 (2009).
16. Bao, B., Prasad, A. S., Beck, F. W. J. & Godmere, M. Zinc modulates mRNA levels of cytokines. *Am J Physiol-Endoc M* **285**, E1095–E1102 (2003).
17. Mcmillan, R. M., Macintyre, D. E., Beesley, J. E. & Gordon, J. L. Regulation of macrophage lysosomal enzyme-secretion: role of arachidonate metabolites, divalent-cations and cyclic-amp. *J Cell Sci* **44**, 299–315 (1980).
18. Li, X., Ito, A., Sogo, Y., Wang, X. P. & LeGeros, R. Z. Solubility of Mg-containing beta-tricalcium phosphate at 25 degrees C. *Acta Biomater* **5**, 508–517 (2009).
19. Ito, A. *et al.* Resorbability and solubility of zinc-containing tricalcium phosphate. *J Biomed Mater Res* **60**, 224–231 (2002).
20. Ito, A., Ojima, K., Naito, H., Ichinose, N. & Tateishi, T. Preparation, solubility, and cytocompatibility of zinc-releasing calcium phosphate ceramics. *J Biomed Mater Res* **50**, 178–183 (2000).
21. Wang, X. P. *et al.* Mesoporous bioactive glass coatings on stainless steel for enhanced cell activity, cytoskeletal organization and AsMg immobilization. *J Mater Chem* **20**, 6437–6445 (2010).
22. Wang, X. P. *et al.* Ascorbate-apatite composite and ascorbate-FGF-2-apatite composite layers formed on external fixation rods and their effects on cell activity in vitro. *Acta Biomater* **5**, 2647–2656 (2009).
23. Wang, X. P., Ito, A., Sogo, Y., Li, X. & Oyane, A. Zinc-containing apatite layers on external fixation rods promoting cell activity. *Acta Biomater* **6**, 962–968 (2010).
24. Wang, X., Ito, A., Li, X., Sogo, Y. & Oyane, A. Signal molecules-calcium phosphate coprecipitation and its biomedical application as a functional coating. *Biofabrication* **3**, 022001 (2011).
25. Wang, X. P., Ito, A., Sogo, Y., Li, X. & Oyane, A. Silicate-apatite composite layers on external fixation rods and in vitro evaluation using fibroblast and osteoblast. *J Biomed Mater Res A* **92A**, 1181–1189 (2010).
26. Kanzaki, N., Onuma, K., Treboux, G., Tsutsumi, S. & Ito, A. Inhibitory effect of magnesium and zinc on crystallization kineyics of hydroxyapatite (0001) face. *J Phys Chem B* **104**, 4189–4194 (2000).
27. John, E. *et al.* Zinc in innate and adaptive tumor immunity. *J Transl Med* **8**, 118–134 (2010).
28. Kitamura, H. *et al.* Toll-like receptor-mediated regulation of zinc homeostasis influences dendritic cell function. *Nat Immunol* **7**, 971–977 (2006).
29. Sugiura, T., Kuroda, E. & Yamashita, U. Dysfunction of macrophages in metallothionein-knock out mice. *J UOEH* **26**, 193–205 (2004).
30. Lange, T. *et al.* Proinflammatory and osteoclastogenic effects of beta-tricalciumphosphate and hydroxyapatite particles on human mononuclear cells in vitro. *Biomaterials* **30**, 5312–5318 (2009).
31. Sabel, M. S. Cryo-immunology: A review of the literature and proposed mechanisms for stimulatory versus suppressive immune responses. *Cryobiology* **58**, 1–11 (2009).
32. Berinstein, N. L. Enhancing cancer vaccines with immunomodulators. *Vaccine* **25**, B72–B88 (2007).
33. Beadling, C., Johnson, K. W. & Smith, K. A. Isolation of Interleukin-2-Induced Immediate-Early Genes. *P Natl Acad Sci USA* **90**, 2719–2723 (1993).
34. Smith, K. A. Interleukin-2 - Inception, Impact, and Implications. *Science* **240**, 1169–1176 (1988).
35. Old, L. J. Tumor necrosis factor (TNF). *Science* **230**, 630–632 (1985).
36. Helson, L., Green, S., Carswell, E. & Old, L. J. Effect of tumor necrosis factor on cultured human melanoma cells. *Nature* **258**, 731–732 (1975).
37. Watford, W. T., Moriguchi, M., Morinobu, A. & O'Shea, J. J. The biology of IL-12: coordinating innate and adaptive immune responses. *Cytokine Growth F R* **14**, 361–368 (2003).
38. Schoenborn, J. R. & Wilson, C. B. Regulation of interferon-gamma during innate and adaptive immune responses. *Adv Immunol* **96**, 41–101 (2007).
39. Noda, K. *et al.* Phase III double-blind randomized trial of radiation therapy for stage IIIb cervical cancer in combination with low-or high-dose Z-100: Treatment with immunomodulator, more is not better. *Gynecol Oncol* **101**, 455–463 (2006).
40. Wellinghausen, N., Kirchner, H. & Rink, L. The immunobiology of zinc. *Immunol Today* **18**, 519–521 (1997).
41. Wang, X., Li, X., Ito, A., Sogo, Y. & Ohno, T. Pore-size dependent immunogenic activity of mesoporous silica-based adjuvants in cancer immunotherapy. *J Biomed Mater Res A*, http://dx.doi.org/10.1002/jbm.a.34783 (2013).

Acknowledgements

We thank the technical assistance in zeta potential analysis of Dr. Shoichi Nakamura, Otsuka Electronics Co., LTD. This study was supported in part by KAKENHI (Grant-in-Aid for Young Scientists B, No. 23700567 and a Grant-in-Aid for JSPS Fellows, No. 21.09501).

Author contributions

X.W., X.L. and A.I. conceived and designed the study. X.W. and X.L. performed most of the experiments, analyzed data and wrote the paper. K.O. and X.L. prepared and analyzed Figs. 2, 3, S2–S4. Y.S. and T.O. supported the in vitro and in vivo tests. All authors reviewed the manuscript.

Additional information

Supplementary information accompanies this paper at http://www.nature.com/scientificreports

Competing financial interests: The authors declare no competing financial interests.

How to cite this article: Wang, X.P. *et al.* Zn- and Mg- Containing Tricalcium Phosphates-Based Adjuvants for Cancer Immunotherapy. *Sci. Rep.* **3**, 2203; DOI:10.1038/srep02203 (2013).